

# Statistical Discrimination in Learning Agents

Edgar A. Duéñez-Guzmán<sup>1</sup>, Kevin R. McKee<sup>1</sup>, Yiran Mao<sup>1</sup>, Ben Coppin<sup>1</sup>, Silvia Chiappa<sup>1</sup>,  
Alexander S. Vezhnevets<sup>1</sup>, Michiel A. Bakker<sup>1</sup>, Yoram Bachrach<sup>1</sup>, Suzanne Sadedin<sup>2</sup>, William Isaac<sup>1</sup>,  
Karl Tuyls<sup>1</sup> and Joel Z. Leibo<sup>1</sup>

<sup>1</sup>DeepMind, <sup>2</sup>Independent researcher

Undesired bias afflicts both human and algorithmic decision making, and may be especially prevalent when information processing trade-offs incentivize the use of heuristics. One primary example is *statistical discrimination*—selecting social partners based not on their underlying attributes, but on readily perceptible characteristics that covary with their suitability for the task at hand. We present a theoretical model to examine how information processing influences statistical discrimination and test its predictions using multi-agent reinforcement learning with various agent architectures in a partner choice-based social dilemma. As predicted, statistical discrimination emerges in agent policies as a function of both the bias in the training population and of agent architecture. All agents showed substantial statistical discrimination, defaulting to using the readily available correlates instead of the outcome relevant features. We show that less discrimination emerges with agents that use recurrent neural networks, and when their training environment has less bias. However, all agent algorithms we tried still exhibited substantial bias after learning in biased training populations.

## Introduction

Choosing good social partners is one key to successful human cooperation (Henrich, 2017), but accurately evaluating a potential partner requires acquiring, integrating and processing information across a variety of situations (Brosnan and De Waal, 2002; Schino and Aureli, 2009). Information processing trade-offs create pressure to learn and apply cheap heuristics in partner choice (Schino and Aureli, 2010). These heuristics, however, can produce undesired biases. Such biases are evident in both human behavior (Devine, 1989; Greenwald and Banaji, 1995) and machine learning algorithms (Caliskan et al., 2017; Zuiderveen Borgesius et al., 2018), and have clear negative effects on economic efficiency and human wellbeing (Ayres, 1991; Bielby and Baron, 1986; Fang and Moro, 2011; Li et al., 2020; Maitzen, 1991; Schwab, 1986). However, the process of their development has not been widely studied.

One formalism used to understand the emergence of such heuristics is *statistical discrimination*. Statistical discrimination occurs when a decision maker must assess an individual’s suitability as a partner but lacks immediate access to features that are causally relevant to that choice. Instead the decision maker bases its assessment on features that are readily available and, in their experience, correlate with the ones of interest (Arrow, 1972; Phelps, 1972). Statistical discrimination stands in contrast to taste-based discrimination, where decision makers have an intrinsic preference for one group over another (Guryan and Charles, 2013).

Models of statistical discrimination do not attempt to capture the full complexity of racial, gender, and other types of discrimination in human societies, which likely involve a wide range of cognitive phenomena such as *in-group favoritism* (Balliet et al., 2014), *group entitativity* (Yzerbyt et al., 1998), and more. Nonetheless, it is possible that multi-generational patterns of systematic social exclusion could be initiated and/or supported by statistical discrimination (Arrow, 1998).

Traditional statistical discrimination models assume a decision maker evaluates a referent indi-

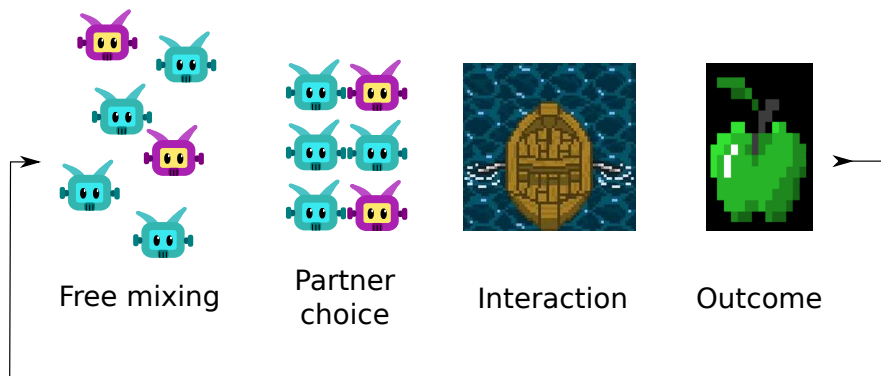


Figure 1 | Cooperative iterations follow a pattern of repeated phases: During free mixing, individuals have access to observable features, but not directly their suitability as partners. Individuals form pairs based on what information is available to them and proceed to interact. The outcome of the interaction is a pair of payoff (or rewards) assigned to the individuals in a pair.

vidual in a one-shot interaction where only perceptible information is available. In reality, decision makers can improve their knowledge of the outcome-relevant characteristics of social partners in a gradual manner. For instance, even in the employment setting where statistical discrimination was originally formulated by [Arrow \(1972\)](#), employers in the real world refine their assessment of job applicants with successive filters and stages. Employers use résumé screening, multiple rounds of interviews, internships and other provisional employment opportunities to improve their knowledge of the applicant’s suitability for a job. In other words, real-world situations are temporally extended, require acquiring, processing and integrating information across time, and comprise a complex tapestry of uncertainty, repeated interactions, and risk management. Limits to time, information processing ability, or the reliability of signals of partner quality will therefore impact the accuracy of decision making, and produce higher bias. Yet, there currently exist no theoretical models to understand the interplay of such limits.

In this work, we introduce a new game theoretical framework for statistical discrimination which advances the state-of-the-art in three ways: (i) allows for sequential decision making; (ii) provides individuals with the ability to choose their partners; and (iii) allows for evaluation of partners based on direct or indirect experience. We then validate this model on a temporally and spatially extended multiagent reinforcement learning environment where agents with varying information processing abilities engage in repeated social interactions with partner choice.

### Reinforcement learning as a model of human behavior

Recently, multiagent reinforcement learning (MARL) has emerged as a framework for the study of social interactions ([Kleiman-Weiner et al., 2016](#); [Leibo et al., 2017](#); [Peysakhovich and Lerer, 2018](#); [Tuyls and Noeé, 2005](#)) by generalizing traditional models of social behaviour to more realistic scenarios in two important ways. First, it enables study of more complex environments than the ones covered by traditional game theory methods; the environments can be spatial, and temporally extended, grounding the abstract conceptions of actions and interactions in a rich world. Second, it enables the study of agents in those rich environments whose decision processes are limited by learning algorithms and information processing ability, and whose interactions are grounded by the laws of their worlds.

In contrast to many game theoretic models that assume optimal behaviour, models of bounded rationality explore the role of limited information processing ability and biases ([Simon, 1957](#)) in the

dynamics and behaviors of a population. MARL offers a fresh approach to modeling bounded rationality, focusing on the learning dynamics, where the bounds are implicit to the learning process (Leibo et al., 2017; McKee et al., 2021).

MARL has been used to study a variety of social situations, including social dilemmas (Hughes et al., 2018; Leibo et al., 2017; Lerer and Peysakhovich, 2017), norm and convention formation (Bakker et al., 2021; Köster et al., 2020; Lerer and Peysakhovich, 2019), communication (Foerster et al., 2016; Lazaridou et al., 2020), and many more. A recent article explored partner choice in an abstract iterated social dilemma environment (Anastassacos et al., 2020), validating that partner choice can indeed promote cooperation in learning agents.

### Partner choice in human societies

Partner choice is a critical mechanism for cooperation in nature (Barclay and Willer, 2007; Fu et al., 2008; Noë and Hammerstein, 1994), and evaluation of social partners is postulated as a major driving force in human evolution (Dunbar, 1998). Previous theoretical work has established that partner choice is a mechanism that can promote cooperation (Gintis et al., 2008; Santos et al., 2006). Ostracism has been observed to promote and maintain cooperation in cultural contexts ranging from hunter gatherers and small-scale pastoral societies (Söderberg and Fry, 2016), to ancient Athenians (Ouwkerk et al., 2005), as well as in experimental studies of contemporary Westerners (Feinberg et al., 2014). Given its cross-cultural ubiquity, it is plausible that evolved cognitive mechanisms for partner choice contribute to systemic social exclusion (Kurzban and Leary, 2001; Tooby and Cosmides, 1988).

Due to limits of cognition and information processing, the mechanisms involved in partner choice may go beyond the (rational but undesirable) statistical discrimination and end up being applied irrationally. This is especially likely where social evaluations are rapid; humans make more mistakes when making decisions under time pressure (Rubinstein, 2013), and these results transfer to social interactions (Evans et al., 2015) including in responses to discrimination (FitzGerald and Hurst, 2017; Greenwald and Banaji, 1995). In primates, there is evidence that reciprocity is driven by relatively simple cognitive processes (Brosnan and De Waal, 2002; Schino and Aureli, 2010). In humans, *implicit bias* is a measurable and unconscious process that biases perception of social partners based on their perceived group membership (Greenwald and Banaji, 1995). Reduction of implicit bias is possible, but appears to require awareness of the bias, and a conscious effort to diminish it (Devine et al., 2012) (cf. (Lai et al., 2016)).

### A model of discrimination with partner choice

We abstract the scenario of choosing desirable social partners to engage in potentially mutually beneficial interactions as an iterated game. Each iteration consists of several phases (see Figure 1). A *free mixing* phase where individuals can observe some characteristics of others that might or might not correlate with actual performance. Crucially, the actual partner quality cannot be directly observed in this phase. A *partner choice* phase where individuals pair up, and commit to interact to the exclusion of all other possible social partners. After choosing partners, the pairs continue to the *interaction* phase, where the outcome relevant behaviors are expressed. The *outcome* phase assigns payoffs (or rewards) to each of the individuals based on how they, and their partner, behaved during the interaction phase.

Iterated social dilemmas are the dominant framework to study the dynamics of social relationships (Axelrod and Hamilton, 1981; Nowak and May, 1992). They consist of a population of individuals engaging in repeated pair-wise social interactions. We extend this framework by introducing partner

choice (Hauk, 2001; Stanley et al., 1993). For simplicity, we assume that if both individuals in a pair were happy with the outcome of their previous interaction, they can and will be able to pair up again at the next partner choice phase. Individuals can choose to unilaterally end a relationship by simply choosing someone else. In addition to observing the outcome of their immediate interaction, individuals might be able to observe the outcomes of other interactions in the population. Constraining an individual’s access to their outcomes, or the outcomes of other pairs, is how we model information processing ability in our analytical model. In the reinforcement learning model, this ability to perceive and process outcomes of interactions between other individuals is grounded on the observations of the environment (see Section ).

As is typical in iterated social dilemmas, we model interactions as a(n instantaneous) matrix game. In an interaction, each individual has access to two strategies: *cooperate* or *defect*. Individuals then simultaneously choose one strategy, and receive a payoff depending on a payoff matrix  $A$ . In this work we use the payoff matrix of *Stag Hunt* (Rousseau, 2009; Skyrms, 2001),

$$\begin{array}{cc} & \begin{array}{cc} C & D \end{array} \\ \begin{array}{c} C \\ D \end{array} & \left( \begin{array}{cc} R & S \\ T & P \end{array} \right) \end{array} \quad (1)$$

where  $R > T \geq P > S$ . An individual playing strategy  $i$  interacting with one playing strategy  $j$  receives payoff  $A_{i,j}$ . So, for instance, if both individuals cooperate, both get the payoff  $R$ , whereas if only the first one cooperates, they get  $S$ , and their partner gets  $T$ .

We chose *Stag Hunt* instead of the *Prisoner’s Dilemma* as the underlying dynamics of the social interactions because our focus here is on situations where cooperation is prevalent in the population. The emergence and maintenance of cooperation has been extensively studied elsewhere (Fletcher and Doebeli, 2009; Henrich et al., 2010; Nowak, 2006)). In contrast to the *Prisoner’s Dilemma* where there is always an incentive to defect, the incentive in *Stag Hunt* is to coordinate with your partner. Mutual cooperation is preferred over mutual defection, and once mutual cooperation has been achieved, there is no incentive to deviate. Because of these properties, *Stag Hunt* is regarded as better capturing the dynamics of long term cooperation (Skyrms, 2004).

Individuals have a set of perceptible attributes that may or may not correlate with the strategy they play during an interaction. We consider a focal individual living through  $k$  social iterations. We assume a basic level of rationality, that is, they would not choose to defect or end a relationship when they are in a mutually cooperative partnership. We model their different levels of rationality based on their ability to react to the behaviour of their partners, the behaviours of other individuals in the population, and the specific partner sampling strategy they employ. In particular, we consider two broad types of behaviors: *unconditional*, which either cooperates or defects, regardless of partner, and never ends relationships; and *reciprocating*, which cooperates when partner cooperates, otherwise ends the relationship. We also consider two partner sampling styles: *visual*, which samples exclusively based on perceptible attributes; and *aware*, which samples first based on perceptible attributes, but observes all interactions in the population, thereafter, samples cooperators exclusively.

Intuitively, an unconditional behavior is less sophisticated than a reciprocating one. And reciprocating behaviors that rely on *visual* sampling are less cognitively demanding than ones with *aware* sampling. We also refer to an *omniscient* behavior which is provided as an upper-bound, representing the maximum possible payoff. An omniscient individual knows the outcome-relevant features, and ignores any other information.

We denote by  $\rho$  the probability that, on the first interaction, the focal individual chooses a partner that cooperates. This quantity depends on a wide range of factors, including the individual’s partner choice policy, the population composition, and the correlation between perceptible features and

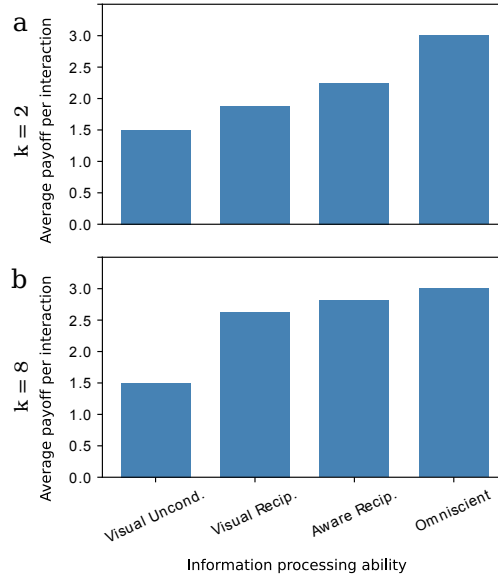


Figure 2 | The relationship between individual behavior and payoff in the analytical model for few iterations ( $k = 2$ ) (a) and more iterations ( $k = 8$ ) (b). The  $x$ -axis also maps to the ability of the individual to use available information, with the lowest ability being on the left, and the highest on the right. Payoffs are computed with  $\rho = 0.5, R = 3, T = P = 1, S = 0$ . More sophisticated behaviors (and thus, those requiring more sophisticated information processing) achieve higher reward.

behaviors. This quantity allows us to write the payoffs of individuals expressing different policies in a compact and intuitive way. For a full explanation of this quantity and how it maps to individuals' information processing abilities, please refer to the Supplementary Material.

Behaviours and sampling styles are largely orthogonal, except that an *unconditional aware* individual would be hard to distinguish from a *visual aware* one. Therefore, we only consider the following four policies:

1. **Visual unconditional:** samples partners of only one color, and unconditionally cooperates with them ( $\pi_{VU}$ ).
2. **Visual reciprocator:** samples partners of only one color, cooperates first with them, but ends the relationship if they defect ( $\pi_{VR}$ ).
3. **Aware reciprocator:** samples first a partner of a specific color and cooperates with them, if they defect, exclusively samples cooperators from then on (the individual is aware of the behaviors of others from the second iteration) ( $\pi_{AR}$ ).
4. **Omniscient:** always samples cooperators and cooperates with them ( $\pi_O$ ).

which stand in as our buckets for the information processing of individuals, from low to high, respectively.

The total payoff over  $k$  iterations of these strategies are:

$$\mathcal{U}_k(\pi_{VU}) = k(\rho R + (1 - \rho)S) \quad (2)$$

$$\mathcal{U}_k(\pi_{VR}) = kR - \frac{1 - \rho}{\rho} \left(1 - (1 - \rho)^k\right) (R - S) \quad (3)$$

$$\mathcal{U}_k(\pi_{AR}) = (k - 1)R + \rho R + (1 - \rho)S \quad (4)$$

$$\mathcal{U}_k(\pi_O) = kR, \quad (5)$$

which, for sufficiently large  $k$ , imply

$$\mathcal{U}_k(\pi_{VU}) < \mathcal{U}_k(\pi_{VR}) < \mathcal{U}_k(\pi_{AR}) < \mathcal{U}_k(\pi_O) \quad (6)$$

Figure 2 shows averages of these equations when the interaction is driven by the payoff matrix (1), with the chance of sampling a cooperater  $\rho = 0.5$ , for  $k = 2$  iterations and  $k = 8$ . For full derivations, please refer to the Supplementary Material.

Our model shows, via the inequalities in (6), that an individual’s payoff increases with its ability to process information about others. Less discriminatory behavior results in higher payoff. Finally, from equations (2–5), the higher the number of iterations,  $k$ , the larger the potential benefit of making partner choices based on actual outcome data, rather than perceptible features (contrast Figure 2a with Figure 2b).

## Reinforcement learning model

To test the insights from the theoretical model presented above, we create a multiagent reinforcement learning model that captures the properties of iterated interactions with partner choice. The environment is spatially and temporally extended, and information about the outcomes of interactions with partners and between third parties is perceptual.

### Boat race environment

The environment is inspired by the boat rowing thought experiment posed by Hume (Hume, 2012), considered as a golden example of *Stag Hunt* (See Figure 3a). In our environment, 6 players engage in a back and forth series of boat races across a river to reach apples that confer a reward. Boats, however, cannot be rowed by a single player, and thus, players need to find a partner before each race and coordinate their rowing during the race to cross the river. When the players are on the boat, they can choose from two different rowing actions at each timestamp: *paddle*, that is efficient, but costly if not coordinated with its partner; and *flail*, that is inefficient, but isn’t affected by the partner’s action. When both players *paddle*, the boat moves one cell every 3 timesteps. When either player *flails*, the boat has a 10% probability of moving one cell, and a reward penalty of  $-0.5$  is given to its partner if that partner is currently *paddling* (i.e. if they have executed the paddle action within the last 3 timesteps).

Two perceptible attributes are given to distinguish players (see Figure 3b). First, every player is colored purple or teal. The color is readily observable as the players perceive their environment as an RGB image window around themselves (see Figure 3a), but is insufficient to individualize a player’s behavior. Second, a *badge*, is given to every player at the start of the episode, which uniquely identifies them within the episode. The badge is a pattern of  $2 \times 2$  dark gray or white pixels at the center of the player’s sprite. The badge is not persistent across episodes.

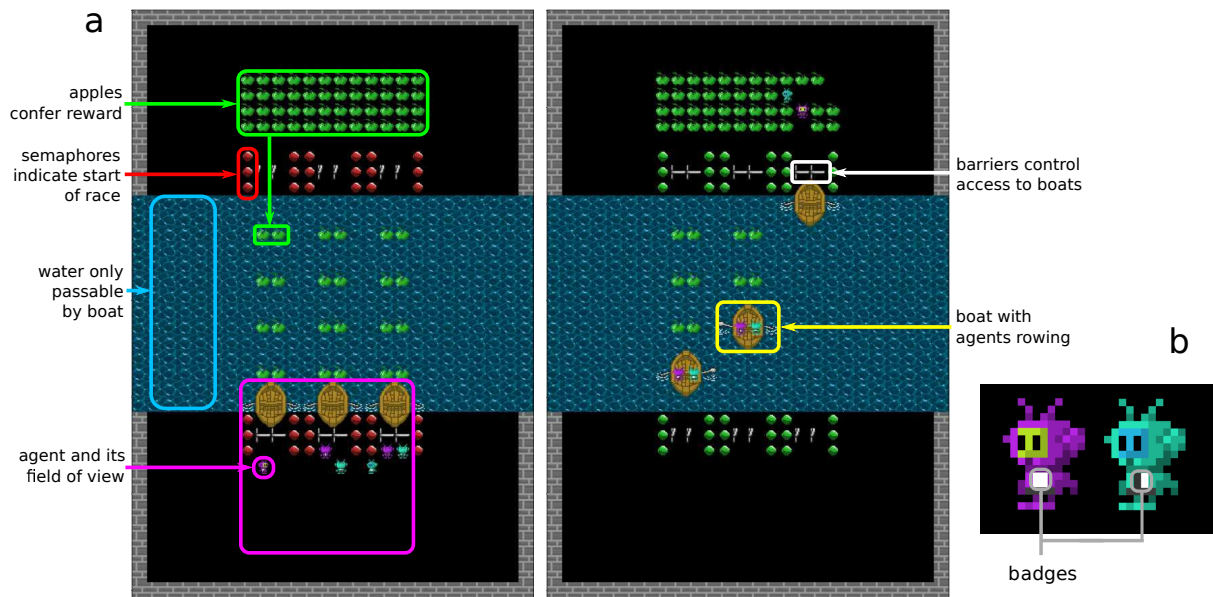


Figure 3 | The *boat race* environment. (a) Six players (teal and purple) pair up to row boats (brown) and cross the river to access apples (green) that confer rewards. Agents can move freely on the river banks (black) but cannot walk across the river (water sprites in blue). Access to the boats is gated by barriers (gray). On the left we see a frame from before a race starts (semaphores are red) and agents are able to move freely. On the right we see a frame from after the race has started. The semaphores have turned green, and the barriers lifted to provide access to the boats. (b) Avatars are assigned a unique random “badge” at the beginning of an episode so their identity can be known throughout the episode.

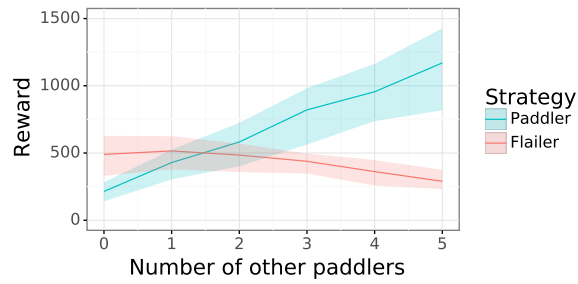


Figure 4 | The Schelling diagram of the *boat race* environment with 8 races ( $k = 8$ ), unconditional cooperation (paddler), and defection (flailer). Depicted are the expected payoffs (average in solid line, quartiles in shaded area) that an individual joining an episode with a particular number of paddlers (on the  $x$ -axis) would obtain, depending on their choice of strategy (paddler or flailer).

An episode consists of a number  $k$  of discrete races of equal duration. At the beginning of each race, access to the boats is blocked by barriers. The barriers lift after a predetermined amount of time, giving the players time to move freely and approach the boat or partner of their choice (like the “free mixing” phase, see Figure 1). The topology of the environment is such that once a pair of players is behind the barriers of a boat, no other player can force themselves into that boat (this corresponds to the “partner choice” phase). If a player so wishes, however, they can back away and walk to another boat. Once a player reaches a seat, they remain seated until either they reach the other river bank, or the time allotted for the race is up, in which case they are disqualified and removed for the rest of the episode (the “interaction” phase).

In the environment there are apples that provide reward to the players that touch them. The apples are consumed in the process, but will be replenished eventually (see below). They are positioned in two different locations: along the river to encourage progress; and on the opposite river bank from the players, as a reward for finishing the race (the “outcome” phase).

The apples on the river are replenished at the start of each race. The apples on the river bank replenish at a constant rate, but disappear altogether when the race time is up (and re-appear on the opposite bank). The replenishing rate of the apples on the river bank is high enough that not even the 6 players optimally consuming them can exhaust them. Therefore, there is a strong incentive to finish a race quickly, so as to accrue the largest reward. For full details see the Supplementary Material.

**Possible policies.** The environment admits behaviors that implement the policies from the theoretical model. A *visual unconditional* would pair up with agents of one color, when available, or at random when not, and always paddle. A *visual reciprocator* would pair on the first race with an agent of one color if available. If their partner (mostly) paddled during the race, they would remember their badge and pair with them in subsequent races. If the partner (mostly) flailed, they would look for another partner of that color, if available. An *aware reciprocator* would pair on the first race with an agent of one color, if available. During the race, this agent would look at the badges of all the players, and infer whether they are flailing or paddling based on their rowing pattern and boat speed. From the second race, it would exclusively pair with cooperators, if available.

## Environment validation

To verify that our environment has the properties of an iterated *Stag Hunt*, we compute in Figure 4 its *Schelling diagram* (Pérolat et al., 2017; Schelling, 1973). It is possible to read off various game theoretic properties from a Schelling diagram including whether a game is a social dilemma. A



Schelling diagram is a plot that summarizes the incentives of a set of players who face a binary choice of a strategy to pursue. In our case the choice of strategy is either always paddle (paddler), or always flail (flailer). The way to interpret the Schelling diagram is to consider a focal individual joining an episode where there are a certain number of paddlers, and the rest are flailers (for a total of 5 other players). This focal individual then faces a binary choice of whether to join as a paddler, and receive the payoff that paddlers receive given the group composition, or receive the payoff of flailers. For instance, if the episode has 3 paddlers, and 2 flailers already, the focal player joining as a paddler would receive the payoff of the paddler’s line at  $x = 3$  in Figure 4 (on average  $\approx 800$  reward), and if joining as a flailer would receive the payoff of the flailer’s line at  $x = 3$  (on average  $\approx 490$ ). Therefore, if there are 3 paddlers already in the environment, there is an incentive to join as a paddler.

To obtain paddlers and flailers, we train A3C agents (Espeholt et al., 2018; Mnih et al., 2016) with a preferred rowing type. We give a pseudo-reward of +5 for executing their preferred rowing type, and of -5 for executing the wrong rowing type. All other rewards are left intact. We validated that paddlers overwhelmingly "paddle" when in the boat, while flailers "flail" (see Supplementary Material).

From Figure 4, we can see that when paddlers are abundant, paddling is advantageous, however, when paddlers are rare, flailing is advantageous, which correspond to a population version of *Stag Hunt* (as per the definition proposed in (Hughes et al., 2018)). Thus, we can refer to paddlers as *cooperators* and flailers as *defectors*.

## Training and evaluation of agents

Now that we know that the boat race environment has the right incentive structure, we proceed to train and evaluate reinforcement learning agents. Like in the theoretical model case, we consider a focal agent training in a *community* of other agents. To form the training community of a focal agent, we freeze the parameters of the agents from the Schelling diagram, and refer to them as *bots*. Bots are of one of four types: purple cooperators, purple defectors, teal cooperators, or teal defectors. We will refer to the focal agent as a *naive learner* to differentiate them from the bots in the community. Naive learners can be of either color, and have no intrinsic preference for either type of rowing.

**Training.** A training community consists of 20 bots:  $n$  purple cooperators,  $n$  teal defectors,  $10 - n$  purple defectors and  $10 - n$  teal cooperators, for  $n = 0, \dots, 10$ . Therefore, there are 11 possible community compositions. Notice that a training community will always have 10 cooperators (and defectors), and 10 purple (teal) bots. What changes between compositions is the statistical association of color with strategy, and we will refer to this as the *community bias*. Naive learners will be assigned to a particular community, and train in episodes with 5 bots sampled (without replacement) from their training community.

We train naive learners with four different architectures: A3C with and without an LSTM (Espeholt et al., 2018), and V-MPO with and without an LSTM (Song et al., 2019). We chose these architectures to reflect different information processing abilities: LSTM provides agents with memory which can be used to reciprocate previous partner cooperation; V-MPO is a more advanced agent than A3C and is expected to learn better. For each agent architecture we train one naive learner of each color for each of the 11 possible community compositions. We also have two values for the number of races  $k$ : 2 and 8. Therefore, in total, we train 44 ( $= 2 \times 11 \times 2$ ) agents of each architecture. These videos ([youtu.be/vweO6k6cx5E](https://youtu.be/vweO6k6cx5E) and [youtu.be/nYbiQyT5Rxs](https://youtu.be/nYbiQyT5Rxs)) show episodes of a V-MPO naive learner with an LSTM for 2 and 8 races respectively. To improve interpretability, we post-process the video to highlight the naive learner in white, cooperator bots in blue, and defector bots in red.

**Evaluation.** For each naive learner, we ran 50 *test* episodes with a new *test* community that had no community bias (i.e. color and strategy are uncorrelated). This testing community was composed of held out bots that had trained in the same number of races as the naive learner but it has not interacted with at training. Therefore, any partner choice observed is due to zero-shot transfer to co-players.

The *association matrix*  $P$  of a naive learner is a  $2 \times 2$  matrix of counts where  $P_{i,j}$  corresponds to the number of times the naive learner shared a boat with a bot with color  $i \in p, t$  (for purple and teal, respectively) and strategy  $j \in c, d$  (for cooperators and defectors, respectively). For instance,  $P_{t,d}$  corresponds to the number of times the naive learner associated with a teal defector. We define the *participation* of an agent as the sum of the entries in their association matrix  $P$ . We define the *discrimination index* of a naive learner as

$$\mathcal{D} = |P_{p,c} - P_{t,c}| + |P_{p,d} - P_{t,d}| - |P_{p,c} - P_{p,d}| - |P_{t,c} - P_{t,d}|$$

This index measures the difference between how much an agent is associating by color:  $|P_{p,c} - P_{t,c}| + |P_{p,d} - P_{t,d}|$  (sum of absolute differences across rows); versus how much it is associating by behavior:  $|P_{p,c} - P_{p,d}| + |P_{t,c} - P_{t,d}|$  (sum of absolute differences across columns). A positive value means the agent prefers to associate with bots based on their color rather than their behavior. A negative value means they prefer to associate by behavior rather than color. A value of zero means that they oversample a color, only insofar as they oversample a behavior (i.e. there isn't a row or a column that is larger element-wise than the other, see Supplementary Material).

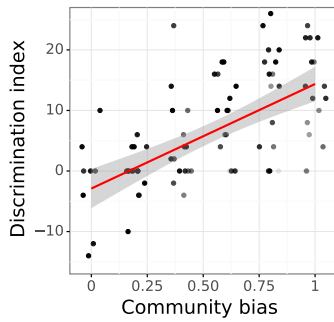
**Estimated CO<sub>2</sub> emissions.** Experiments were conducted using an internal GPU cluster with carbon efficiency of 0.27 kgCO<sub>2</sub>eq/kWh. A cumulative of 30,000 hours of computation was performed on Tesla P100 GPUs (TDP of 250W). Total emissions are estimated at 2025 kgCO<sub>2</sub>eq, all of which were directly offset. Estimations were conducted using the [Machine Learning Impact calculator \(Lacoste et al., 2019\)](#).

## Results

To understand the policy that the naive learners are executing, we keep track of their association matrix, and what type of rowing they engage in. Naive learners overwhelmingly paddle, but when paired with a defector, they flail or do not row at all (see Supplementary Material). We also tested if the agents (both naive learners and bots) had any preference for a particular seat (left or right), or boat (left, middle, or right), but they did not (see Supplementary Material). Thus we can infer that any association between particular individuals is a result of explicit partner choice, either of themselves or others.

To understand the extent to which an agent is using information about their partners during an episode, we track the discrimination index on the first and last races. 95% confidence intervals for the discrimination index range from  $(-48.0, -28.0)$  for an agent with perfect information who exclusively prefers one strategy, to  $(28.0, 48.0)$  for an agent who exclusively prefers one color. A naive learner sampling at random has a discrimination index within  $(-10, 10)$  with 95% confidence (see Supplementary Material).

To evaluate the effect that the training community bias has on the learned behavior of naive learners, we plot the test time discrimination index, as described in Section , as a response of the training community bias that the naive learner experienced. The left panel of Figure 5 shows this plot where each point represents averages of 50 test episodes for a single naive learner. Agents trained



LSTM	$k$	Race	Discr. index
No	2	first	17.838710
No	2	last	21.379032
No	8	first	8.717742
No	8	last	13.153226
Yes	2	first	17.750000
Yes	2	last	14.129032
Yes	8	first	6.798387
Yes	8	last	4.629032

Figure 5 | **Left:** Discrimination index as a response to training community bias. Plot corresponds to A3C naive learners without an LSTM on their last race of 8. Other cases show a similar response (see Supplementary Material). Each point shows average values over 50 episodes in unbiased test communities. The shading of the points represents the naive learner’s participation (light is less participation, dark is more). We plot the best fit linear regression (red line) with bootstrapped 95% confidence intervals (gray shaded region). **Right:** Discrimination index in the first and last races for agents with and without LSTM, for 2 or 8 races. Agents trained in 8 races discriminate less overall, agents without LSTM discriminate more in the last race, while agents with LSTM discriminate less.

in an unbiased community exhibit a slight negative discrimination index in the last race, whereas agents trained in highly biased communities universally have positive discrimination.

Notice that in the case of  $k = 8$  races, in principle agents have enough opportunity to sample each of their 5 co-players each in one race, leaving enough leeway to partner with cooperators in the last race, if any are available. In the case of  $k = 2$  races, sampling a cooperator in the last race requires either sampling a cooperator by luck on the first race, and remembering to partner with them in the last race, or, more generally, observing the behaviours of other agents and inferring their policy based on their performance. The environment allows for this type of deduction, as the information is available even though it is challenging to keep track of.

Agents trained in highly biased communities tend to exhibit high discrimination at testing time. This is unlikely only due to competition for the preferred partners since the effect changed with the training community bias, and agents were never observed to associate by behavior as much as they associate by color (their discrimination index was never very negative, see Figure 5, and the Supplementary Material).

The discrimination index of the RL agents increases roughly linearly with their training community’s bias (Figure 5, left). This is in contrast to predictions from the analytical model, where any detectable bias should be maximally exploited by reward maximizers. As a consequence, we would have expected more of a threshold response to increases in training community bias.

Only agents with an LSTM were able to have a lower discrimination index in their last race than their first one (Figure 5, right). However, none of our agents were able to robustly ignore the correlation between color and behaviour at test time, even in the most favorable case: a V-MPO agent with LSTM, in 8 races. Importantly, this is not because agents are unable to effectively realize their partner choice preferences, since agents from highly biased communities were indeed able to associate by color effectively, and often within the confidence interval of optimal association (by color). Agents trained on 8 races discriminated less than those trained in 2 races (Figure 5, right). This suggests that the incentives to discriminate can be reduced through repeated interactions.

## Limitations

By design, we limit the scope of this work to that of statistical discrimination. Our work tackles one particular aspect of discrimination that we can study directly with the tools currently available because it does not require predictions or assumptions about multi-generational dynamics on human societies. In doing so, we are able to make a clear and formal contribution, but also limit the possible impact that our insights can have on the societal problems at large. Statistical discrimination is almost certainly a factor within societal discrimination, but the effect size of this factor is unknown.

The results discussed here do not, nor they attempt to, claim to solve the complex problems of racism, sexism, ableism, etc; nor of representation of specific or implied groups of people. These problems require a multi-faceted approach, and no one aspect is likely to resolve them outright. Finally, while reinforcement learning agents are a model of human behavior and learning, they are far from perfect. They are better able to capture spatial and temporally complex behaviors than traditional rational economic models and evolutionary agent-based models of behavior, but are still far from the richness of the human brain.

## Discussion

Our theoretical model shows that agents have an incentive to statistically discriminate on the basis of perceptible features when their training environment is biased (i.e. the perceptible features are correlated with the quality of social partners). This effect intensifies if they are unable to obtain, process, or incorporate the information of which other agents are good social partners. Agents that choose partners based on their direct quality not only perform better overall, but also discriminate less. This pattern held true in the multiagent reinforcement learning model.

Past research has shown that unfair biases arising in supervised learning models can be mitigated via precautions with training data and model deployment (Dixon et al., 2018; Mehrabi et al., 2019; Zhang et al., 2018). Here, we found that reinforcement learning agents trained in a biased community were unable to avoid statistical discrimination. This was expected for agents without an LSTM, for whom reciprocating strategies are likely inaccessible. More surprisingly, it was also true for agents with an LSTM.

Agents with an LSTM are, in principle, able to remember previous social partners in an episode, and thus we expected them to engage in reciprocation, either *visual reciprocation* (associating by color in the first race, but then filter undesirable partners until finding a suitable partner of the preferred color), or *aware reciprocation* (associating by color in the first race, but paying close attention to all interactions and only associating with cooperators in any subsequent races). To our surprise, all agents, regardless of the presence or absence of an LSTM, consistently failed to pair with cooperators even in the last race, maintaining a high discrimination index. This discrimination was not due to an inability to enact partner choices, since agents trained in extremely biased communities exhibited a discrimination index at evaluation that was near the theoretical maximum.

Agents with an LSTM, while unable to fully de-bias themselves, were nonetheless able to discriminate less in the last race than in the first one. This suggests that the ability to process and incorporate information plays a central role in how individuals learn to choose a partner in a non-discriminatory way. This effect, however, was far from optimal, and all agents, with or without an LSTM, behaved closer to the theoretical prediction of *visual unconditional* players (Equation 2) than even *visual reciprocators* (Equation 3). None of them came even close to exhibiting an *aware* partner sampling (Equation 4), even though that information was available in their observations. Mitigating unfair biases in end-to-end reinforcement learning systems may require new safeguards designed with this

in mind.

**Interventions on the agent.** It might be possible to modify RL agents to explicitly ameliorate discrimination. However, such interventions would typically require privileged knowledge of the world (for example, the true causal graph of color, behavior, and its influence on reward). The goal of this work is (by choice) not to attempt to solve discrimination, but to propose a framework to study its emergence in learning agents, particularly when they do not have exhaustive mechanisms to deal with discrimination. It is unrealistic to assume that we would be able to enumerate and (manually or automatically) correct all potential sources of bias. We decided to focus on this goal as we believe that shedding light on the emergence of discrimination, an area that is still very poorly understood, is a necessary first step for devising sensible approaches to alleviating this problem.

**Fairness in machine learning.** The study of undesired biases in machine learning systems is an active area of research, ranging from formalizing desiderata for system evaluation to the development of methods for mitigating undesired biases (Barocas et al., 2019; Chouldechova and Roth, 2020; Gajane and Pechenizkiy, 2017; Mehrabi et al., 2019; Mitchell et al., 2018; Verma and Rubin, 2018). These efforts have focused predominantly on static prediction settings where only the immediate impact of a decision is taken into account. However, when repeated interactions are not properly accounted for, systems that seem fair in a static sense might exacerbate harmful biases over time (Liu et al., 2018; Zhang et al., 2020). Awareness of this issue has motivated a surge of research on fairness in sequential decision making settings, including work on bandits and reinforcement learning (Jabbari et al., 2017; Joseph et al., 2016), as well as on simulation of fairness interventions and causal modelling (Creager et al., 2020; D’Amour et al., 2020).

Work on fairness in machine learning has made a distinction between *group-level fairness* and *individual-level fairness*. Group fairness ensures some form of parity (e.g. between positive outcomes, or errors) across different protected groups (split by e.g. gender). Individual fairness, in contrast, is concerned with constraints that bind on the level of an individual, for example by requiring “similar” people to receive similar outcomes (Dwork et al., 2012). Our work, framed as statistical discrimination, studies how bias emerges and persists and how this violates fairness at the level of an individual. However, while (with some exceptions e.g. (Zhang and Shah, 2014)) most of the literature is concerned with decisions made by one entity (such as e.g. a bank on an individual), this work considers decentralized interactions among peers (Chouldechova and Roth, 2020).

**Insights.** Our work suggests two general ways to reduce discrimination: one is to decrease the bias in the training community; and the second is through more careful evaluation of potential partners.

In our setting, theory predicts that small decreases in community bias will have no effect in the policy learned. Individuals will still have an incentive to sample a color exclusively when available. Interestingly, our agents do not conform to that prediction. They instead respond to small reductions in community bias by learning a proportionally less discriminatory policy. We posit that this is due to the stochasticity of sampling co-players for an episode from a community, which results in a bet-hedging solution on the part of the agent. Essentially, whether an agent uses a signal depends on its reliability, and so as the signal becomes more reliable, it becomes more exploitable. This pattern is compatible with the phenomenon observed in the field of ML fairness where reducing bias in the training data has been observed to have a positive impact in the fairness metrics of classification algorithms (Kamiran and Calders, 2012). It is also compatible with the *contact hypothesis* which postulates that stereotype-disconfirming interactions reduce prejudice in humans (Allport et al., 1954; Paluck et al., 2019).

Our results may also be understood within a dual process framework, which posits that slow and deliberative processes may override automatic habit-like processes. Dual process models have a long history in psychology and neuroscience (reviewed in (Dayan, 2009)). For example in human vision, feedforward decision-making operates rapidly (Greenwald and Banaji, 1995; Thorpe et al., 1996) and may learn dedicated threat-related features (Chekroud et al., 2014), whereas deliberative processes such as mental rotation unfold sequentially via recurrent processing (Lamme and Roelfsema, 2000), and are consequently much slower (Shepard and Metzler, 1971). These differences parallel the contrast between our purely feedforward agents and ones with LSTM.

A related comparison arises between model-based (MB) and model-free (MF) reinforcement learning (Daw et al., 2005). Whereas MB learning can prospectively plan to achieve desired outcomes using knowledge of the likely consequences of actions, MF learning gradually updates cached values of actions retrospectively from experience (Akam et al., 2015; Dayan and Daw, 2008). When outcome values change, model-based decision-makers can rapidly change their behavior, whereas model-free decision-makers need additional repetitions (Dickinson, 1985). In the human brain, MF learning (for example, of habits and rituals) is associated with the dorsolateral striatum (Graybiel, 2008) while MB learning is associated with persistent activity in the prefrontal cortex (Daw et al., 2005; Wang et al., 2018). By allowing agents to learn relevant features from experience when the task demands it, LSTMs may offer a model for the neural mechanisms that underlie MB learning (Wang et al., 2018). In our model, agents with LSTMs benefited from incorporating individual-oriented information for partner choice, whereas feed-forward networks were incapable of this and thus continued to discriminate. These observations suggest that engaging different neurological systems may modulate the impact of statistical discrimination.

Discrimination, in all its forms, is a key societal issue. Only by disentangling the factors contributing to its emergence, establishment, and maintenance can we hope to solve this problem. This work contributes to the understanding of the emergence of bias, and serves as evidence that using reinforcement learning systems in combination with traditional analytical tools can provide insights into important societal issues.

## References

- Thomas Akam, Rui Costa, and Peter Dayan. 2015. Simple Plans or Sophisticated Habits? State, Transition and Learning Interactions in the Two-Step Task. *PLOS Computational Biology* 11, 12 (2015), 1–25.
- Gordon Willard Allport, Kenneth Clark, and Thomas Pettigrew. 1954. *The nature of prejudice*. Addison-wesley Reading, MA.
- Nicolas Anastassacos, Stephen Hailes, and Mirco Musolesi. 2020. Partner selection for the emergence of cooperation in multi-agent systems using reinforcement learning. In *Proceedings of the AAAI Conference on Artificial Intelligence*, Vol. 34(05). 7047–7054.
- Kenneth J. Arrow. 1972. Some mathematical models of race discrimination in the labor market. *Racial discrimination in economic life* (1972), 187–204.
- Kenneth J. Arrow. 1998. What has economics to say about racial discrimination? *Journal of economic perspectives* 12, 2 (1998), 91–100.
- Robert Axelrod and William D. Hamilton. 1981. The evolution of cooperation. *Science* 211, 4489 (1981), 1390–1396. <https://doi.org/10.1126/science.7466396>  
arXiv:<https://science.sciencemag.org/content/211/4489/1390.full.pdf>

- Ian Ayres. 1991. Fair driving: Gender and race discrimination in retail car negotiations. *Harvard Law Review* (1991), 817–872.
- Michiel A. Bakker, Richard Everett, Laura Weidinger, Iason Gabriel, William S. Isaac, Joel Z. Leibo, and Edward Hughes. 2021. Modelling Cooperation in Network Games with Spatio-Temporal Complexity. In *Proceedings of the 20th International Conference on Autonomous Agents and MultiAgent Systems (Virtual Event, United Kingdom) (AAMAS '21)*. International Foundation for Autonomous Agents and Multiagent Systems, Richland, SC, 1455–1457.
- Daniel Balliet, Junhui Wu, and Carsten KW De Dreu. 2014. Ingroup favoritism in cooperation: A meta-analysis. *Psychological bulletin* 140, 6 (2014), 1556.
- Pat Barclay and Robb Willer. 2007. Partner choice creates competitive altruism in humans. *Proceedings of the Royal Society B: Biological Sciences* 274, 1610 (2007), 749–753.
- Solon Barocas, Moritz Hardt, and Arvind Narayanan. 2019. *Fairness and Machine Learning*. fairml-book.org. <http://www.fairmlbook.org>.
- Charles Beattie, Thomas Köppe, Edgar A Duéñez-Guzmán, and Joel Z Leibo. 2020. DeepMind Lab2D. *arXiv preprint arXiv:2011.07027* (2020).
- William T Bielby and James N Baron. 1986. Men and women at work: Sex segregation and statistical discrimination. *American journal of sociology* 91, 4 (1986), 759–799.
- Sarah F. Brosnan and Frans B. M. De Waal. 2002. A proximate perspective on reciprocal altruism. *Human Nature* 13, 1 (2002), 129–152.
- Aylin Caliskan, Joanna J Bryson, and Arvind Narayanan. 2017. Semantics derived automatically from language corpora contain human-like biases. *Science* 356, 6334 (2017), 183–186.
- Adam Mourad Chekroud, Jim A. C. Everett, Holly Bridge, and Miles Hewstone. 2014. A review of neuroimaging studies of race-related prejudice: does amygdala response reflect threat? *Frontiers in Human Neuroscience* 8 (2014), 179.
- Alexandra Chouldechova and Aaron Roth. 2020. A snapshot of the frontiers of fairness in machine learning. *Commun. ACM* 63, 5 (2020), 82–89.
- Elliot Creager, David Madras, Toniann Pitassi, and Richard Zemel. 2020. Causal modeling for fairness in dynamical systems. In *International Conference on Machine Learning*. PMLR, 2185–2195.
- Alexander D’Amour, Hansa Srinivasan, James Atwood, Pallavi Baljekar, D Sculley, and Yoni Halpern. 2020. Fairness is not static: deeper understanding of long term fairness via simulation studies. In *Proceedings of the 2020 Conference on Fairness, Accountability, and Transparency*. 525–534.
- Nathaniel D. Daw, Yael Niv, and Peter Dayan. 2005. Uncertainty-based competition between prefrontal and dorsolateral striatal systems for behavioral control. *Nature neuroscience* 8, 12 (2005), 1704–1711.
- Peter Dayan. 2009. Goal-directed control and its antipodes. *Neural Networks* 22, 3 (2009), 213–219.
- Peter Dayan and Nathaniel D. Daw. 2008. Decision theory, reinforcement learning, and the brain. *Cognitive, Affective, & Behavioral Neuroscience* 8, 4 (2008), 429–453.
- Patricia G. Devine. 1989. Stereotypes and prejudice: Their automatic and controlled components. *Journal of personality and social psychology* 56, 1 (1989), 5.

- Patricia G. Devine, Patrick S. Forscher, Anthony J. Austin, and William T. L. Cox. 2012. Long-term reduction in implicit race bias: A prejudice habit-breaking intervention. *Journal of experimental social psychology* 48, 6 (2012), 1267–1278.
- Anthony Dickinson. 1985. Actions and habits: the development of behavioural autonomy. *Philosophical Transactions of the Royal Society of London. B, Biological Sciences* 308, 1135 (1985), 67–78.
- Lucas Dixon, John Li, Jeffrey Sorensen, Nithum Thain, and Lucy Vasserman. 2018. Measuring and mitigating unintended bias in text classification. In *Proceedings of the 2018 AAAI/ACM Conference on AI, Ethics, and Society*. 67–73.
- Robin I. M. Dunbar. 1998. The social brain hypothesis. *Evolutionary Anthropology: Issues, News, and Reviews: Issues, News, and Reviews* 6, 5 (1998), 178–190.
- Cynthia Dwork, Moritz Hardt, Toniann Pitassi, Omer Reingold, and Richard Zemel. 2012. Fairness through awareness. In *Proceedings of the 3rd innovations in theoretical computer science conference*. 214–226.
- Lasse Espeholt, Hubert Soyer, Remi Munos, Karen Simonyan, Vlad Mnih, Tom Ward, Yotam Doron, Vlad Firoiu, Tim Harley, Iain Dunning, et al. 2018. Impala: Scalable distributed deep-rl with importance weighted actor-learner architectures. In *International Conference on Machine Learning*. PMLR, 1407–1416.
- Anthony M. Evans, Kyle D. Dillon, and David G. Rand. 2015. Fast but not intuitive, slow but not reflective: Decision conflict drives reaction times in social dilemmas. *Journal of Experimental Psychology: General* 144, 5 (2015), 951.
- Hanming Fang and Andrea Moro. 2011. Theories of statistical discrimination and affirmative action: A survey. *Handbook of social economics* 1 (2011), 133–200.
- Matthew Feinberg, Robb Willer, and Michael Schultz. 2014. Gossip and ostracism promote cooperation in groups. *Psychological science* 25, 3 (2014), 656–664.
- Chloë FitzGerald and Samia Hurst. 2017. Implicit bias in healthcare professionals: a systematic review. *BMC medical ethics* 18, 1 (2017), 1–18.
- Jeffrey A. Fletcher and Michael Doebeli. 2009. A simple and general explanation for the evolution of altruism. *Proceedings of the Royal Society B: Biological Sciences* 276, 1654 (7 Jan. 2009), 13–19. <https://doi.org/10.1098/rspb.2008.0829>
- Jakob N. Foerster, Yannis M. Assael, Nando De Freitas, and Shimon Whiteson. 2016. Learning to communicate with deep multi-agent reinforcement learning. *arXiv preprint arXiv:1605.06676* (2016).
- Feng Fu, Christoph Hauert, Martin A. Nowak, and Long Wang. 2008. Reputation-based partner choice promotes cooperation in social networks. *Physical Review E* 78, 2 (2008), 026117.
- Pratik Gajane and Mykola Pechenizkiy. 2017. On formalizing fairness in prediction with machine learning. *arXiv:1710.03184*
- Herbert Gintis, Joseph Henrich, Samuel Bowles, Robert Boyd, and Ernst Fehr. 2008. Strong reciprocity and the roots of human morality. *Social Justice Research* 21, 2 (2008), 241–253.
- Ann M. Graybiel. 2008. Habits, rituals, and the evaluative brain. *Annu. Rev. Neurosci.* 31 (2008), 359–387.



- Anthony G. Greenwald and Mahzarin R. Banaji. 1995. Implicit social cognition: attitudes, self-esteem, and stereotypes. *Psychological review* 102, 1 (1995), 4.
- Jonathan Guryan and Kerwin Kofi Charles. 2013. Taste-based or statistical discrimination: the economics of discrimination returns to its roots. *The Economic Journal* 123, 572 (2013), F417–F432.
- Esther Hauk. 2001. Leaving the prison: Permitting partner choice and refusal in prisoner’s dilemma games. *Computational Economics* 18, 1 (2001), 65–87.
- Joseph Henrich. 2017. *The secret of our success: How culture is driving human evolution, domesticating our species, and making us smarter*. Princeton University Press.
- Joseph Henrich, Jean Ensminger, Richard McElreath, Abigail Barr, Clark Barrett, Alexander Bolyanatz, Juan C. Cardenas, Michael Gurven, Edwina Gwako, Natalie Henrich, Carolyn Lesorogol, Frank Marlowe, David Tracer, and John Ziker. 2010. Markets, Religion, Community Size, and the Evolution of Fairness and Punishment. *Science* 327, 5972 (19 March 2010), 1480–1484. <https://doi.org/10.1126/science.1182238>
- Matteo Hessel, Hubert Soyer, Lasse Espeholt, Wojciech Czarnecki, Simon Schmitt, and Hado van Hasselt. 2019. Multi-task deep reinforcement learning with popart. In *Proceedings of the AAAI Conference on Artificial Intelligence*, Vol. 33(01). 3796–3803.
- Edward Hughes, Joel Z. Leibo, Matthew G. Phillips, Karl Tuyls, Edgar A. Duéñez-Guzmán, Antonio García Castañeda, Iain Dunning, Tina Zhu, Kevin R. McKee, and Raphael et. al. Koster. 2018. Inequity aversion improves cooperation in intertemporal social dilemmas. *arXiv preprint arXiv:1803.08884* (2018).
- David Hume. 1739/2012. *A treatise of human nature*. Courier Corporation.
- Shahin Jabbari, Matthew Joseph, Michael Kearns, Jamie Morgenstern, and Aaron Roth. 2017. Fairness in reinforcement learning. In *International Conference on Machine Learning*. PMLR, 1617–1626.
- Max Jaderberg, Volodymyr Mnih, Wojciech Marian Czarnecki, Tom Schaul, Joel Z Leibo, David Silver, and Koray Kavukcuoglu. 2016. Reinforcement learning with Unsupervised Auxiliary Tasks. *arXiv preprint arXiv:1611.05397* (2016).
- Matthew Joseph, Michael Kearns, Jamie Morgenstern, and Aaron Roth. 2016. Fairness in learning: classic and contextual bandits. In *Proceedings of the 30th International Conference on Neural Information Processing Systems*. 325–333.
- Faisal Kamiran and Toon Calders. 2012. Data preprocessing techniques for classification without discrimination. *Knowledge and Information Systems* 33, 1 (2012), 1–33.
- Max Kleiman-Weiner, Mark K Ho, Joseph L Austerweil, Michael L Littman, and Joshua B Tenenbaum. 2016. Coordinate to cooperate or compete: abstract goals and joint intentions in social interaction. In *CogSci*.
- Raphael Köster, Kevin R. McKee, Richard Everett, Laura Weidinger, William S. Isaac, Edward Hughes, Edgar A. Duéñez-Guzmán, Thore Graepel, Matthew Botvinick, and Joel Z. Leibo. 2020. Model-free conventions in multi-agent reinforcement learning with heterogeneous preferences. *arXiv preprint arXiv:2010.09054* (2020).
- Robert Kurzban and Mark R. Leary. 2001. Evolutionary origins of stigmatization: the functions of social exclusion. *Psychological bulletin* 127, 2 (2001), 187.

- Alexandre Lacoste, Alexandra Luccioni, Victor Schmidt, and Thomas Dandres. 2019. Quantifying the Carbon Emissions of Machine Learning. *arXiv preprint arXiv:1910.09700* (2019).
- Calvin K Lai, Allison L Skinner, Erin Cooley, Sohad Murrar, Markus Brauer, Thierry Devos, Jimmy Calanchini, Y Jenny Xiao, Christina Pedram, Christopher K Marshburn, et al. 2016. Reducing implicit racial preferences: II. Intervention effectiveness across time. *Journal of Experimental Psychology: General* 145, 8 (2016), 1001.
- Victor A. F. Lamme and Pieter R. Roelfsema. 2000. The distinct modes of vision offered by feedforward and recurrent processing. *Trends in neurosciences* 23, 11 (2000), 571–579.
- Angeliki Lazaridou, Anna Potapenko, and Olivier Tieleman. 2020. Multi-agent communication meets natural language: Synergies between functional and structural language learning. *arXiv preprint arXiv:2005.07064* (2020).
- Joel Z. Leibo, Vinicius Zambaldi, Marc Lanctot, Janusz Marecki, and Thore Graepel. 2017. Multi-agent Reinforcement Learning in Sequential Social Dilemmas. In *Proceedings of the 16th International Conference on Autonomous Agents and Multiagent Systems (AA-MAS 2017)*. Sao Paulo, Brazil.
- Adam Lerer and Alexander Peysakhovich. 2017. Maintaining cooperation in complex social dilemmas using deep reinforcement learning. *arXiv preprint arXiv:1707.01068* (2017).
- Adam Lerer and Alexander Peysakhovich. 2019. Learning existing social conventions via observationally augmented self-play. In *Proceedings of the 2019 AAI/ACM Conference on AI, Ethics, and Society*. 107–114.
- Danielle Li, Lindsey R. Raymond, and Peter Bergman. 2020. *Hiring as Exploration*. Technical Report. National Bureau of Economic Research.
- Lydia T. Liu, Sarah Dean, Esther Rolf, Max Simchowitz, and Moritz Hardt. 2018. Delayed Impact of Fair Machine Learning. In *Proceedings of the 35th International Conference on Machine Learning*. 3150–3158.
- Michael W Macy and Andreas Flache. 2002. Learning dynamics in social dilemmas. *Proceedings of the National Academy of Sciences* 99, suppl 3 (2002), 7229–7236.
- Stephen Maitzen. 1991. The ethics of statistical discrimination. *Social Theory and Practice* 17, 1 (1991), 23–45.
- Kevin R. McKee, Edward Hughes, Tina O. Zhu, Martin J. Chadwick, Raphael Koster, Antonio García Castaneda, Charlie Beattie, Thore Graepel, Matt Botvinick, and Joel Z. Leibo. 2021. Deep reinforcement learning models the emergent dynamics of human cooperation. *arXiv preprint arXiv:2103.04982* (2021).
- Ninareh Mehrabi, Fred Morstatter, Nripsuta Saxena, Kristina Lerman, and Aram Galstyan. 2019. A survey on bias and fairness in machine learning. *arXiv preprint arXiv:1908.09635* (2019).
- Shira Mitchell, Eric Potash, Solon Barocas, Alexander D’Amour, and Kristian Lum. 2018. Prediction-based decisions and fairness: A catalogue of choices, assumptions, and definitions. *arXiv:1811.07867*
- Volodymyr Mnih, Adria Puigdomenech Badia, Mehdi Mirza, Alex Graves, Timothy Lillicrap, Tim Harley, David Silver, and Koray Kavukcuoglu. 2016. Asynchronous methods for deep reinforcement learning. In *International conference on machine learning*. PMLR, 1928–1937.

- Ronald Noë and Peter Hammerstein. 1994. Biological markets: supply and demand determine the effect of partner choice in cooperation, mutualism and mating. *Behavioral ecology and sociobiology* 35, 1 (1994), 1–11.
- Martin A. Nowak. 2006. Five Rules for the Evolution of Cooperation. *Science* 314, 5805 (08 Dec. 2006), 1560–1563. <https://doi.org/10.1126/science.1133755>
- Martin A. Nowak and Robert M. May. 1992. Evolutionary games and spatial chaos. *Nature* 359, 6357 (16 Jan. 1992), 826–9. <https://doi.org/10.1038/355250a0>
- Aaron van den Oord, Yazhe Li, and Oriol Vinyals. 2018. Representation Learning with Contrastive Predictive Coding. *arXiv preprint arXiv:1807.03748* (2018).
- Jaap W. Ouwkerk, Norbert L. Kerr, Marcello Gallucci, and Paul A. M. Van Lange. 2005. Avoiding the social death penalty: Ostracism and cooperation in social dilemmas. *The social outcast: Ostracism, social exclusion, rejection, and bullying* (2005), 321–332.
- Elizabeth Levy Paluck, Seth A. Green, and Donald P. Green. 2019. The contact hypothesis re-evaluated. *Behavioural Public Policy* 3, 2 (2019), 129–158. <https://doi.org/10.1017/bpp.2018.25>
- Julien Pérolat, Joel Z. Leibo, Vinícius Flores Zambaldi, Charles Beattie, Karl Tuyls, and Thore Graepel. 2017. A multi-agent reinforcement learning model of common-pool resource appropriation. In *Advances in Neural Information Processing Systems 30: Annual Conference on Neural Information Processing Systems 2017, December 4-9, 2017, Long Beach, CA, USA*. 3643–3652. <https://proceedings.neurips.cc/paper/2017/hash/2b0f658cbffd284984fb11d90254081f-Abstract.html>
- Alexander Peysakhovich and Adam Lerer. 2018. Towards ai that can solve social dilemmas. In *2018 AAAI Spring Symposium Series*.
- Edmund S. Phelps. 1972. The Statistical Theory of Racism and Sexism. *The American Economic Review* 62, 4 (1972), 659–661.
- Anatol Rapoport, Albert M Chammah, and Carol J Orwant. 1965. *Prisoner's dilemma: A study in conflict and cooperation*. Vol. 165. University of Michigan press.
- Jean-Jacques Rousseau. 2009. *Discourse on Inequality: On the Origin and Basis of Inequality Among Men*. The Floating Press.
- Ariel Rubinstein. 2013. Response time and decision making: An experimental study. *Judgment & Decision Making* 8, 5 (2013).
- Francisco C. Santos, Jorge M. Pacheco, and Tom Lenaerts. 2006. Cooperation prevails when individuals adjust their social ties. *PLoS computational biology* 2, 10 (20 Oct. 2006), e140+. <https://doi.org/10.1371/journal.pcbi.0020140>
- Thomas C. Schelling. 1973. Hockey helmets, concealed weapons, and daylight saving: A study of binary choices with externalities. *Journal of Conflict resolution* 17, 3 (1973), 381–428.
- Gabriele Schino and Filippo Aureli. 2009. Reciprocal altruism in primates: partner choice, cognition, and emotions. *Advances in the Study of Behavior* 39 (2009), 45–69.
- Gabriele Schino and Filippo Aureli. 2010. Primate reciprocity and its cognitive requirements. *Evolutionary Anthropology: Issues, News, and Reviews* 19, 4 (2010), 130–135.

- Stewart Schwab. 1986. Is statistical discrimination efficient? *The American Economic Review* 76, 1 (1986), 228–234.
- Roger N. Shepard and Jacqueline Metzler. 1971. Mental rotation of three-dimensional objects. *Science* 171, 3972 (1971), 701–703.
- Herbert A. Simon. 1957. *Models of man; social and rational*. Wiley.
- Brian Skyrms. 2001. The stag hunt. In *Proceedings and Addresses of the American Philosophical Association*, Vol. 75. JSTOR, 31–41.
- Brian Skyrms. 2004. *The stag hunt and the evolution of social structure*. Cambridge University Press.
- Patrik Söderberg and Douglas P. Fry. 2016. Anthropological aspects of ostracism. In *Ostracism, exclusion, and rejection*. Routledge, 268–282.
- H Francis Song, Abbas Abdolmaleki, Jost Tobias Springenberg, Aidan Clark, Hubert Soyer, Jack W Rae, Seb Noury, Arun Ahuja, Siqi Liu, Dhruva Tirumala, et al. 2019. V-MPO: On-policy maximum a posteriori policy optimization for discrete and continuous control. *arXiv preprint arXiv:1909.12238* (2019).
- E Stanley, Dan Ashlock, and Leigh Tesfatsion. 1993. Iterated prisoner’s dilemma with choice and refusal of partners. (1993).
- Simon Thorpe, Denis Fize, and Catherine Marlot. 1996. Speed of processing in the human visual system. *nature* 381, 6582 (1996), 520–522.
- John Tooby and Leda Cosmides. 1988. The evolution of war and its cognitive foundations. *Institute for evolutionary studies technical report* 88, 1 (1988), 1–15.
- Karl Tuyls and Ann Noë. 2005. Evolutionary game theory and multi-agent reinforcement learning. *The Knowledge Engineering Review* 20, 1 (2005), 63–90.
- Sahil Verma and Julia Rubin. 2018. Fairness definitions explained. In *IEEE/ACM International Workshop on Software Fairness*.
- Jane X. Wang, Zeb Kurth-Nelson, Dharshan Kumaran, Dhruva Tirumala, Hubert Soyer, Joel Z. Leibo, Demis Hassabis, and Matthew Botvinick. 2018. Prefrontal cortex as a meta-reinforcement learning system. *Nature neuroscience* 21, 6 (2018), 860–868.
- Vincent Y. Yzerbyt, Anouk Rogier, and Susan T. Fiske. 1998. Group entitativity and social attribution: On translating situational constraints into stereotypes. *Personality and Social Psychology Bulletin* 24, 10 (1998), 1089–1103.
- Brian Hu Zhang, Blake Lemoine, and Margaret Mitchell. 2018. Mitigating unwanted biases with adversarial learning. In *Proceedings of the 2018 AAAI/ACM Conference on AI, Ethics, and Society*. 335–340.
- Chongjie Zhang and Julie A. Shah. 2014. Fairness in Multi-Agent Sequential Decision-Making. In *Advances in Neural Information Processing Systems*, Vol. 27.
- Xueru Zhang, Ruibo Tu, Yang Liu, Mingyan Liu, Hedvig Kjellström, Kun Zhang, and Cheng Zhang. 2020. How do fair decisions fare in long-term qualification?. In *Advances in Neural Information Processing Systems*.
- Frederik Zuiderveen Borgesius et al. 2018. *Discrimination, artificial intelligence, and algorithmic decision-making*. Technical Report. Council of Europe.

## Supplementary material

### Analytical model

We assume a population of individuals that engage in pair-wise repeated interactions for up to  $k$  steps. Each individual has a perceptible attribute  $c \in C$ , a partner sampling policy  $\sigma$ , and a behavior policy  $\pi$ . We assume the set of perceptible attributes  $C$  is discrete, and will be referred to as *colors*. Both the sampling policy  $\sigma$  and the behavior policy  $\pi$  can depend on the perceptible attributes, the history of past interactions with a particular individual, or even on hidden information like the behavior policy of other individuals.

In each interaction, individuals play a symmetric game with two strategies  $C$  and  $D$  corresponding to *cooperation* and *defection*, respectively. The payoff of the game is given by a matrix with two rows ( $C$  and  $D$ ) corresponding to the strategies available to the focal agent, and two columns ( $C$  and  $D$  also) corresponding to the strategies of the co-interactant. The payoff matrix is given by

$$\begin{array}{cc} & \begin{array}{cc} C & D \end{array} \\ \begin{array}{c} C \\ D \end{array} & \left( \begin{array}{cc} R & S \\ T & P \end{array} \right) \end{array}$$

where  $R$  represents the *reward* of mutual cooperation,  $S$  represents the *sucker's* reward,  $T$  represents the *temptation* to defect, and  $P$  is the *punishment* reward for mutual defection (Rapoport et al., 1965). In social dilemmas, there is an incentive to defect, either as a temptation from mutual cooperation, or as risk-avoidance from mutual defection, or both. For Stag Hunt,  $R > T \geq P > S$ , which implies there is no temptation to defect once there is mutual cooperation, but there is a risk-avoidance incentive to defect. This is sometimes referred to as a lack of *greed* and presence of *fear* (Macy and Flache, 2002). Notice that the payoff matrix need not be symmetric. The term symmetric in *symmetric game* refers to the symmetry of player roles and strategy payoff, rather than the properties of the matrix itself.

### Behavior policy

The behavior policy  $\pi$  determines both if the relationship should continue or end; and the strategy to play in the next interaction. When the relationship ends, a new partner will be sampled and this interaction will not count towards the  $k$  steps. Formally,

$$\pi : \mathcal{H} \rightarrow \Delta\{C, D, \Omega\}$$

where  $\mathcal{H}$  is the set of all possible information states available to the individual, and (as discussed above) can include histories of interactions with current and past partners, revealed information about non-partners, and even hidden information about individuals. And  $\Delta\{C, D, \Omega\}$  is the set of probabilities over the two strategies  $C$  and  $D$ , and the termination action  $\Omega$ . We use the notation  $\pi(h)_X$  to denote the probability of playing strategy  $X$  given the history  $h$  and the color of the partner  $c$ . In practice, we often consider deterministic policies, in which case we use the strategy itself as the output of the policy (e.g.  $\pi(h) = C$ ). The special action  $\Omega$  denotes the end of a relationship.

### Partner sampling policy

A partner sampling policy  $\sigma$  determines the next individual to interact with. This function can represent a completely uniform sample over all individuals, or sampling exclusively individuals with a particular color, and even an oracle that always samples a cooperator. We will restrict what information can be used in a sampling function as a stand-in for an individual's ability to process and incorporate information. So, an individual that has no memory will only have access to the color of

other individuals, while an omniscient individual will have access to even the private information of other individuals from the start. There are many other possibilities in between, and we will discuss some later on.

In many cases, we will assume that every time an individual samples a new interaction partner, it is one they have never interacted with before<sup>1</sup>. Formally,  $\sigma$  is a function mapping populations to distributions over populations, i.e.

$$\sigma : \mathcal{H} \rightarrow \Delta\mathcal{P}$$

where  $\Delta X := \{(z_x)_{x \in X} : \sum_{x \in X} z_x = 1, z_x \in [0, 1] \forall x \in X\}$  is the set of all probability distributions over the discrete set  $X$ . Thus, we use  $\sigma(\cdot)_p$  to denote the probability of sampling individual  $p$ .

We define  $\rho$  as the probability that a sampled individual will cooperate in the interaction. Formally, for a focal individual with information state  $h$  let  $\mathcal{G}(h) = \{p \in \mathcal{P} | \pi_p(h') = C\}$  be the subset of the population that will cooperate in the next interaction with the focal individual. Then

$$\rho = \sum_{p \in \mathcal{G}(h)} \sigma(\cdot)_p$$

Individuals don't have access to  $\rho$ , but it can be used to abstract out all the complexities of partner choice and express an individual's payoff in its terms.

In practice, we will restrict ourselves to 3 different partner sampling functions:

A *visual* function which takes into account only the color of the individuals in the population. Always samples partners of the color with the highest probability of cooperation (i.e.  $\arg \max_c \rho$  for  $\mathcal{G}(c)$ ).

A *aware* function that samples like the visual function on the first interaction, but on any subsequent partner samplings, it selects always a cooperator (i.e.  $\rho$  is the same as the one for visual on the first interactions, and  $\rho = 1$  for all interactions after the first one). This is representing an individual who is initially unaware of the other individuals' policies, but after one interaction with *any* individual, it observes the policy of *all* individuals. This is an extreme case of an individual that is not cheating (in the sense of having access to hidden information of other individuals), but is able to observe and infer correctly all information of all other interactions in the population at the first opportunity.

Finally, an *omniscient* function that always samples a cooperator (i.e.  $\rho = 1$  always). This is a cheating individual, and is used only to provide the upper bound on possible performance.

### Broad behavior classes

For the purposes of this article, we will focus on assessing only two extreme classes of behaviors. *Unconditional behaviors*, where the information state comprises only the color  $c$  (i.e.  $\pi_U$  is only a function of  $c$ ). And *reciprocating behaviors*, where the always starts with cooperation with new relationships, and ends the relationship whenever the partner defects, that is, the strategy ignores color (i.e.  $\pi_R$  is only a function of the partner's strategy in the previous interaction). Formally,

$$\begin{aligned} \pi_R(\emptyset) &= C, \\ \pi_R(h) &= \begin{cases} C & \text{if } h_{-1} \neq D \\ \Omega & \text{otherwise} \end{cases}; \text{ for } h \neq \emptyset, \end{aligned}$$

<sup>1</sup>This simplification enables us to avoid keeping track of the histories of previous interactions inducing a more tractable model. This simplification corresponds to an extreme situation in which when once somebody you have interacted with proves themselves socially-unreliable, you don't ever want to interact with them again.

where  $\pi(\emptyset)$  is the strategy to play in a new interaction (i.e. one with empty history), and  $h_{-1}$  denotes the strategy played by the partner in the previous interaction.

### Individual payoffs

We now focus on the payoff of a focal individual and find out under which conditions each of the broad behaviors above are favoured. Let  $\mathcal{U}_i(h, \sigma, \pi; h', \sigma', \pi')$  be the payoff at step  $i$  of an individual with information state  $h$ , sampling policy  $\sigma$ , and behavior  $\pi$  with a partner with information state  $h'$  and policies  $\sigma'$  and  $\pi'$ . Often, we will omit some or all of the parameters to  $\mathcal{U}_i$  when they are clear from context. We can write  $\mathcal{U}_i$  recursively as

$$\mathcal{U}_i = \mathcal{U}_{i-1} + \begin{cases} \pi'(h')_C \pi(h)_C R + \pi'(h')_C \pi(h)_D T + \\ \pi'(h')_D \pi(h)_C S + \pi'(h')_D \pi(h)_D P & \text{if continuing with same partner} \\ \rho [\pi(h)_C R + \pi(h)_D T] + \\ (1 - \rho) [\pi(h)_C S + \pi(h)_D P] & \text{if resampling partner at step } i \end{cases}$$

**Unconditional behaviors.** For unconditional behaviors against partner color  $c$  we have two possibilities, either unconditional defection  $\pi_{UD} = D$  or unconditional cooperation  $\pi_{UC} = D$ .

If the partner is also using an unconditional behavior using visual partner sampling, the payoffs simplify to

$$\mathcal{U}_k(\pi_{UD}) = \rho kT + (1 - \rho)kP \quad (7)$$

$$\mathcal{U}_k(\pi_{UC}) = \rho kR + (1 - \rho)kS. \quad (8)$$

Observe that whether cooperation or defection yields higher payoff depends solely on  $\rho$  (and thus, indirectly on the sampling function  $\sigma$  and the color of the partner) and the payoff matrix. An individual would prefer to unconditionally cooperate whenever

$$\mathcal{U}_k(\pi_{UC}) > \mathcal{U}_k(\pi_{UD})$$

which, by combining Equations (7) and (8), for unconditional behavior partners happens if and only if

$$\frac{\rho}{1 - \rho} > \frac{P - S}{R - T}$$

This inequality has some interesting properties. The left hand side corresponds to the odds ratio of encountering a cooperator versus a defector when sampling partners. The right hand side is the ratio of payoffs associated with cooperation and defection, against an unknown strategy. This payoffs ratio is the threshold beyond which cooperation is favoured. We refer to this quantity  $\frac{P-S}{R-T}$  as the *stakes of interaction*. For Stag Hunt, where  $R > T$  and  $P > S$ , the stakes are always positive. Since  $0 \leq \rho \leq 1$ , there is always some value of  $\rho$  such that the inequality is satisfied. Note that for the Prisoner's Dilemma, the stakes are negative, which flips the direction of the inequality and makes it unsatisfiable.

Even within the family of unconditional behaviors, it would be payoff-maximising to play different strategies against different colored partners, depending on whether the odds ratio of finding a cooperation ( $\rho/(1 - \rho)$ ) of that color exceed the stakes of the interaction. We will denote this

unconditional strategy that picks the best of  $C$  or  $D$  for each color as  $\pi_U$ . Additionally, the payoff-maximising partner sampling function is simply to sample from the color that has the highest empirical proportion of initial cooperators  $\sigma_U = \arg \max_c p_c$ .

In practice, we will just assume an unconditional cooperator, or unconditional defector policy.

**Reciprocating behaviors.** From here on we assume that partnerships are never ended when agents are in mutual cooperation. This is a reasonable assumption when the dynamics of interactions are governed by a Stag Hunt payoff matrix, because mutual cooperation is both a Nash equilibrium and the collective payoff maximising outcome. Therefore, there isn't any incentive from any partner to end the relationship. And since reciprocators end the relationship immediately upon defection of their partner, this is equivalent to having the choice of partnership ending only on the focal individual, which simplifies the derivations substantially.

If an individual is using a visual sampling function, we can expand and simplify the recursive equation into

$$\begin{aligned} \mathcal{U}_k &= \rho kR + (1 - \rho) [S + \rho(k - 1)R + (1 - \rho) [S + \rho(k - 2)R + \dots]] \\ &= \rho R \left( \sum_{i=0}^{k-1} (k - i)(1 - \rho)^i \right) + (1 - \rho)S \left( \sum_{i=0}^{k-1} (1 - \rho)^i \right) \\ &= \rho R \left( \sum_{i=0}^{k-1} (k - i)(1 - \rho)^i \right) + (1 - \rho)S \left( \frac{1 - (1 - \rho)^k}{\rho} \right) \end{aligned}$$

We can simplify the coefficient of the  $\rho R$  term as follows

$$\begin{aligned} \sum_{i=0}^{k-1} (k - i)(1 - \rho)^i &= \sum_{i=0}^{k-1} \sum_{j=0}^i (1 - \rho)^j \\ &= \sum_{i=0}^{k-1} \frac{1 - (1 - \rho)^{i+1}}{\rho} \\ &= \frac{1}{\rho} \left( k - (1 - \rho) \frac{1 - (1 - \rho)^k}{\rho} \right) \end{aligned}$$

which yields the final equation

$$\mathcal{U}_k = kR - \frac{1 - \rho}{\rho} \left( 1 - (1 - \rho)^k \right) (R - S) \quad (9)$$

If an individual is using an aware sampling function, we simplify further as

$$\mathcal{U}_k = (k - 1)R + \rho R + (1 - \rho)S \quad (10)$$

And with aware sampling, we obtain the theoretical maximum payoff of

$$\mathcal{U}_k = kR \quad (11)$$

### Behavioral dominance

Using the computed payoffs of a focal individual pursuing either unconditional or reciprocating behaviors, we now determine the conditions for reciprocating behaviors to dominate unconditional behaviors, as well as the optimal partner sampling policy for these behaviors.



Notice that the payoff for an omniscient reciprocator is greater than that of an aware reciprocator which in itself is greater than that of a visual reciprocator. Therefore, we only need to compare the payoff of an unconditional behavior with a visual reciprocator.

Formally, reciprocating dominates unconditional behaviors if and only if

$$\begin{aligned} \mathcal{U}_k(\sigma, \pi_R) &> \mathcal{U}_k(\sigma', \pi_U) \iff \\ kR - \frac{1-\rho}{\rho} \left(1 - (1-\rho)^k\right) (R-S) &> \rho'kT + (1-\rho')kP; \text{ and} \\ kR - \frac{1-\rho}{\rho} \left(1 - (1-\rho)^k\right) (R-S) &> \rho'kR + (1-\rho')kS \end{aligned}$$

Now, if there is at least one color with an odds ratio of cooperators above the stakes, then we need only look at the second inequality, which simplifies to

$$\begin{aligned} kR - \frac{1-\rho}{\rho} \left(1 - (1-\rho)^k\right) (R-S) &> \rho'kR + (1-\rho')kS \iff \\ k(1-\rho')(R-S) &> \frac{1-\rho}{\rho} \left(1 - (1-\rho)^k\right) (R-S) \iff \\ k &> \frac{1 - (1-\rho)^k}{\rho} \cdot \frac{1-\rho}{1-\rho'} \end{aligned}$$

which is satisfied for sufficiently large  $k$ .

### Reinforcement learning model

We build an environment called *boat race* using DMLab2D (Beattie et al., 2020), which is a configurable and performant library for creating multi-agent 2D environments. The environment consists of objects and avatars, where each avatar is controlled by a single agent, and the avatars can be used to interact with objects. We will refer to an agent controlling an avatar as a player, and we will refer to a player's actions or observations as they pertain to their avatar.

An episode on the environment consists of a number of races  $k$  that is either 2 or 8. Each race is separated in 3 phases, a partner choice phase lasting 65 steps, a semaphore changing phase lasting 5 steps, and a rowing phase lasting 230 steps. Each race runs in the opposite direction of the previous one, alternating North and South directions.

The objects in the environment are:

- **Apples.** Players entering the same location as the apple consume the apple and receive a reward. The apple will respawn depending on its location: at the end of a race for apples above the river; and with a probability of 10% per step for the apples on the goal river bank.
- **Barriers.** Barriers prevent players from entering their location, and are used to gate access to the boats before the rowing phase of the race starts.
- **Semaphores.** These are impassable objects that show a traffic-light pattern signaling the transition from the partner choice phase to the rowing phase of a race. They are colored red during partner choice, and change to yellow for the 5 steps of the semaphore changing phase, and then to green in the rowing phase of the race.
- **Boat.** Boats have two seats that players can enter. Once a player enters a seat, they control the oar next to it with their rowing actions. Players in a seat cannot move anymore, and all of

their movement actions are no-ops. Boats can only move during the rowing phase of a race, and require two players, one on each seat to move. When a boat reaches the opposite river bank, it automatically disembarks its players into the river bank, past the barriers.

- **Water.** Water is impassable by players on foot (i.e. not in a boat). Boats with players can travel across water.

Episodes start with boats on the South river bank, with no apples on that bank, and its barriers closed. The North bank contains apples and its barriers are open. Once the rowing phase starts, the barriers toggle with the North ones being blocked and the South ones being open. At the beginning of the next race, apples on river banks also toggle, with the South ones appearing, and the North ones disappearing.

Players have movement actions and rowing actions. The players can move in any of the cardinal directions (North, East, South or West), and can also turn 90 degrees left or right. There are two rowing actions: paddle and flail. Rowing actions are considered no-ops when the players are not on a boat seat. Similarly, movement actions are no-ops when players are on a seat. Flailing actions can be executed at every time step, and have a 10% probability (non-cumulative for each player) of moving the boat forward at each time step. Paddling actions have a cool down of 2 steps, meaning the can only be executed every 3 steps. Paddling during the cool down period are considered no-ops. Paddling by a partner during the cool down phase will result in the boat moving 1 cell. Flailing by a partner during the cool down phase results in a reward punishment of  $-0.5$  and the paddling attempt is wasted, and progress can only be made by flailing until the cool down ends.

Players have partial observability of  $11 \times 11$  cells around them, with 5 cell to each side of their position, 1 cell behind, and 9 in front. They perceive their environment as RGB images of size  $176 \times 176 \times 3$  (sprites are  $16 \times 16$ ). Players who do not reach the other side of the river by the end of the race are disqualified and removed from the episode. The agent’s observations in this case are fully black (zeros) and all their actions are no-ops.

Agents have a persistent color across episodes, which is instantiated as an avatar of that color in the level. Avatars can be of two colors: purple (base RGB = (145, 30, 180)) and teal (base RGB = (30, 180, 145)). In addition, the avatar is assigned a random badge for each episode, used to uniquely identify the players, but only within that episode. The badge is a set of 4 pixels that can be either black or white. The color of the agent is more salient than the badge.

Apples on the river banks respawned at a rate of 0.1 per timestep, and confer a reward of +1 to the player who eats them.

### ***Agent details***

All agent architectures had the same size convolutional net with two layers with output channels 16 and 32, with a stride of 8 pixels. The convolutional net was followed by a feedforward net with two layers, both with 64 output units. Agents with LSTM, have a hidden state of size 128, using an unroll length of 100. Agents were trained on mini-batches of data of size 16. V-MPO had a pop-art layer (Hessel et al., 2019) for normalizing the value function. A3C minimized a contrastive predictive coding loss (Oord et al., 2018) in the manner of an auxiliary objective (Jaderberg et al., 2016), which in this case contrasted between nearby time points via LSTM state representations (a standard augmentation in recent work with A3C).

Agents for the training community and the production of the Schelling diagram were trained for  $3 \times 10^8$  steps, whereas naive learners were trained for  $1.5 \times 10^9$  steps. We used a learning rate of  $4 \times 10^{-4}$  for A3C agents and  $1 \times 10^{-4}$  for V-MPO agents.

Agents for the training community and Schelling diagram were incentivized to either unconditionally paddle or unconditionally flail. These agents receive a reward of +5 for every rowing that matches their incentive, and  $-5$  if it didn't. Agents overwhelmingly learned to use their incentivized rowing. Across 350 episodes, paddlers never flailed in either 2 races or 8 races. Flailers paddled only twice out of over 200,000 flailing actions, and only in the case of 2 races. Community bots did not exhibit any significant preference towards a particular boat, or a particular side seat within the boat (see Figure 6).

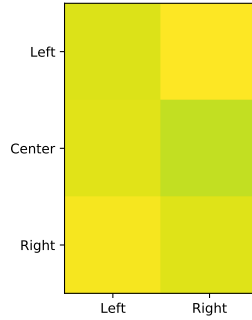


Figure 6 | Physical association of community bots who participated in a race. The figure shows a heat map of the counts for each time a bot was on each of the boats (left, center, right) taking one of the seats (left, right). The values ranged from 220 (darker), to 232 (lighter).

Out of 2,200 episodes used for evaluation for each architecture, we counted the number of times the naive learner paddled and flailed (see Table 1). Given that paddling has a cool down, flailing would be expected to be 3 times as frequent if agents were rowing at random. Naive learners primarily learned to paddle, with the weakest case being the A3C agent with LSTM, where the absolute flailing was greater than the absolute paddling, but only by a factor of two. We also calculated the correlation of the paddling and flailing on the first race of the naive learner with its partner. Overall, there was a positive correlation between the flailing for agents without an LSTM. The rest of the correlations were low (see Table 1).

Architecture	# flail	# paddle	flail corr.	paddle corr.
A3C LSTM	34,062	17,604	0.07	-0.12
A3C no LSTM	19,525	31,217	0.26	0.03
VMPO LSTM	8,767	20,370	0.06	0.10
VMPO no LSTM	18,120	27,756	0.21	-0.02

Table 1 | Counts of the number of paddle actions and the number of flail actions for naive learners as well as the correlation between their rowing and that of their partner. All counts correspond to the first race for a total of 2,200 episodes where the partners were uniformly random across strategy and color.

### Discrimination index

We define the *association matrix*  $P$  of a naive learner as a  $2 \times 2$  matrix of counts where  $P_{i,j}$  corresponds to the number of times the naive learner shared a boat with a bot with color  $i$  and strategy  $j$ . We define the *participation* of an agent as the sum of the entries in their association matrix  $P$ . We define

the *discrimination index* of a naive learner as

$$D = |P_{p,c} - P_{t,c}| + |P_{p,d} - P_{t,d}| - |P_{p,c} - P_{p,d}| - |P_{t,c} - P_{t,d}|$$

For simplicity, let's rename the entries of  $P$  as  $a, b, c$ , and  $d$ . Without loss of generality,  $a > b, c, d$ , thus there are 4 cases:  $c > d \& b > d$ ,  $c > d \& b < d$ ,  $c < d \& b > d$ , or  $c < d \& b < d$ . Note that  $D = 0 \iff a > d > b, c$ . Otherwise  $D = 2(c - b)$  or  $2(c - d)$  or  $2(d - b)$  which is always even.

We simulated an individual sampling partners according to a particular strategy. Figures 7 and 8 show the histogram over 10,000 simulations of an individual sampling uniformly at random, or sampling only based on one color, when present. We assume that the other 5 players are of a random color and random strategy, and that the focal individual always has first choice of partner.

Figures 9 and 10 show the discrimination index as a value of the training community bias, as measured in an unbiased evaluation community. A clear pattern of higher community bias resulting in higher discrimination index is seen throughout.

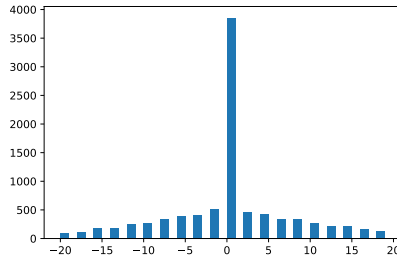


Figure 7 | Histogram of discrimination index for 10,000 simulations of unbiased random sampling of partners.

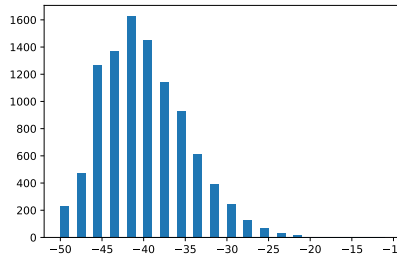


Figure 8 | Histogram of discrimination index for 10,000 simulations of sampling cooperators (uniformly random), if any are available, otherwise, sampling a random partner.

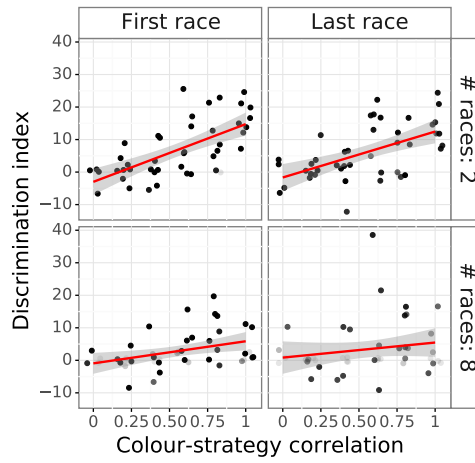


Figure 9 | Discrimination index for agents with an LSTM in the first and last races, for the cases of 2 and 8 races.

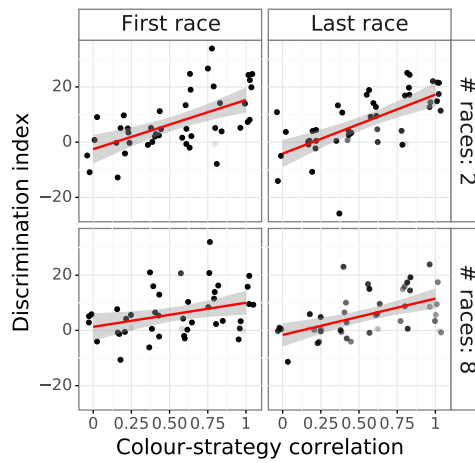


Figure 10 | Discrimination index for agents without an LSTM in the first and last races, for the cases of 2 and 8 races.